Available online at www.sciencedirect.com
ScienceDirect
Polymer 47 (2006) 7601–7606
polymer
www.elsevier.com/locate/polymer

Power law of molecular weight dependence of lateral growth rate of isotactic polypropylene

Koji Yamada [a,*], Kaori Watanabe [b], Kiyoka Okada [c], Akihiko Toda [d], Masamichi Hikosaka [d]

[a] Kawasaki Development Center, SunAllomer Ltd., 2-3-2 Yako, Kawasaki-ku, Kawasaki 210-0863, Japan
[b] Collaborative Research Center, Hiroshima University, 2-313 Kagamiyama, Higashi-Hiroshima 739-8527, Japan
[c] Graduate School of Biosphere Science, Hiroshima University, 1-4-4 Kagamiyama, Higashi-Hiroshima 739-8528, Japan
[d] Graduate School of Integrated Arts and Sciences, Hiroshima University, 1-7-1 Kagamiyama, Higashi-Hiroshima 739-8521, Japan

Received 25 April 2006; received in revised form 24 July 2006; accepted 24 July 2006
Available online 7 September 2006

Abstract

Molecular weight (M) dependence of the lateral growth rate (V) of α form crystal of isotactic polypropylene (iPP) was studied. Reliable equilibrium melting temperature determined in our previous study was used for the analysis of supercooling dependence of V. A power law of M of V, $V \propto M_n^{-H}$, was obtained, where H is a small constant ($H = 0.7$). The small H, which is similar to that of the hexagonal phase of polyethylene ($H = 0.7$) in comparison with the value of $H = 1.7$ for the orthorhombic phase of polyethylene, confirmed our prediction of smaller H for ''rod like'' chain polymers because of easier chain sliding within the interface between the crystalline phase and the melt. Thus, the universality of the important role of topological nature in polymer crystallization was confirmed. Lateral surface free energy (σ) of the α form of iPP was obtained as $\sigma \cong 1.59 \times 10^{-6}$ J/cm^2.

Keywords: Isotactic polypropylene; Molecular weight; Growth rate

1. Introduction

For improving the properties and productivity of industrial polymeric materials, it is important to control the crystallization rate. One of the authors proposed a ''chain sliding diffusion theory'' and showed that polymer crystallization in general should be regarded as a topological process [1–6]. In order to confirm the topological nature of polymer crystallization, it will be essential to examine the molecular weight (M) dependence of linear growth rate (V) of polymer crystals.

The lateral growth of lamellar crystal is regarded as a two-dimensional nucleation process at the growth front. During the process, polymer chains are transported from the melt into the surface region of the crystal. Then, the absorbed chain slides along its axis and disentangles for rearranging within the melt–crystal interface. As a result, a small nucleus grows and becomes stable. The rate of two-dimensional nucleation is experimentally observed as the crystal growth rate, which is expressed by a well-known equation [3,4],

$$V = V_0 \exp\left(-\frac{B}{T\Delta T}\right), \tag{1}$$

where ΔT is the degree of supercooling defined as

$$\Delta T = T_m^0 - T_c, \tag{2}$$

with the equilibrium melting temperature, T_m^0, and the crystallization temperature, T_c. V_0 and B are related to the self-diffusion constant of molecules (D) and to the free energy barrier of a critical nucleus (ΔG^*), respectively, as shown below,

$$V_0 \propto D \tag{3}$$

* Corresponding author. Tel.: +81 44 276 3562; fax: +81 44 266 9432.
E-mail address: koji_yamada@sunallomer.co.jp (K. Yamada).

0032-3861/$ - see front matter © 2006 Elsevier Ltd. All rights reserved.
doi:10.1016/j.polymer.2006.07.077

$$\frac{B}{T\Delta T}=\frac{\Delta G^*}{mkT}=\frac{4b_0\sigma\sigma_e T_m^0/\Delta h_f\Delta T}{mkT}, \quad (4)$$

where k is the Boltzmann constant, m is a constant related to the growth mechanism, *i.e.*, $m=1$ for mono-nucleation of regime I or multi-nucleation of regime III and $m=2$ for multi-nucleation of regime II, b_0 is the thickness of one growth layer, σ is the lateral surface free energy, σ_e is the end surface free energy, and Δh_f is the heat of fusion. Here, the temperature dependence of D is expressed as the Vogel–Fulcher or Williams–Landel–Ferry (WLF) equation [7–9], and hence the dependence of V_0 is given as,

$$V_0=V_0'\exp\left(-\frac{U^*}{R(T_c-T_\infty)}\right), \quad (5)$$

where V_0' is a coefficient, U^* is the effective activation energy related to chain motion, R is the gas constant and T_∞ is the temperature at which chain motion ceases.

As seen in Eq. (4), ΔG^* depends on $\Delta T=T_m^0-T_c$, where T_m^0 depends on M significantly. Therefore, it is important to obtain reliable T_m^0 as a function of M ($T_m^0(M)$) for the determination of M dependence of V. Hoffman et al. [10] examined the M dependence of the coefficient B of polyethylene (PE), based on the $T_m^0(M)$ extrapolated from the melting points of *n*-alkane, known as the Flory–Vrij equation [11]. The coefficient increased with the increase in M for low M, became constant for intermediate M, and became smaller for still higher M. On the other hand, Hikosaka et al. [3,4] also examined the dependence of PE with $T_m^0(M)$ obtained from reliable Gibbs–Thomson plot. They concluded that V_0 depends on M, while B does not [3,4]. As has been discussed by Wunderlich [12] in detail, it is known that T_m^0 of PE obtained by the extrapolation method, T_m^0(FV), and Gibbs–Thomson plot one T_m^0(GT), are different significantly; *e.g.*

$$\begin{aligned} T_m^0(\mathrm{FV}) &= T_m^0(\mathrm{GT})+3.7\mathrm{K} \quad \text{for } M=10^4 \\ &= T_m^0(\mathrm{GT})+5.5\mathrm{K} \quad \text{for } M=10^5. \end{aligned} \quad (6)$$

it means that, for PE of $M=10^5$ crystallized at $T_c\sim 130$ °C, $\Delta T\sim 16$ and 10.5 °C with T_m^0(FV) and T_m^0(GT), respectively. Therefore, the difference in the M dependence of V with different sources of T_m^0 should be caused by the difference in the M dependence of the T_m^0. Thus, the reliability of $T_m^0(M)$ significantly affects the accuracy of the analysis. We think that $T_m^0(M)$ determined by the Gibbs–Thomson method is more reliable because the method is based on correct thermodynamic consideration.

The results of Hikosaka et al. [3,4] indicate that the M dependence of V is determined by the self-diffusion of chain molecules, D, while the nucleation barrier, ΔG^*, is not significantly affected by M. In terms of the M dependence of V_0, the following relationship was obtained,

$$V_0\propto D\propto M^{-H}, \quad (7)$$

where the power H is dependent on the degree of order of crystalline phase, *i.e.*, $H=0.7$ and $H=1.7$ for the hexagonal and orthorhombic phases of PE, respectively.

PE is regarded as a special polymer because of its "planar-zigzag" chain conformation. Most polymers have helical conformations, but the effect of chain conformation on sliding diffusion has not been clarified yet. It is expected that the power, H, of helical polymers will be small, because the sliding diffusion will be easy for rod-like chains in comparison with "planar-zigzag" chains due to small interchain friction among them. In the present study, isotactic polypropylene (iPP) is used as a typical stereoregular polymer. The V of iPP has been studied for many years [13,14], but the M dependence could not been confirmed because of the lack of reliable $T_m^0(M)$. In our previous study, we applied reliable Gibbs–Thomson plot and determined the M dependence of T_m^0 [15–17]. Therefore, it is now possible to evaluate reliable M dependence of V of iPP.

Lateral surface free energy (σ) and end surface free energy (σ_e) are the important parameters determining the crystallization rate. Clark and Hoffman [13] evaluated $\sigma=1.15\times 10^{-6}$ J/cm^2 by using the following semi-empirical equation,

$$\sigma=\alpha\Delta h_f(a_0b_0)^{1/2}, \quad (8)$$

where α is a constant and a_0b_0 is the cross-sectional area of the chain under the assumption of $\alpha=0.1$. They also obtained $\sigma\sigma_e=7.4$–7.9×10^{-12} J^2/cm^4 from the slope of $\log V$ plotted against $(T\Delta T)^{-1}$ and $\sigma_e=6.5$–7.0×10^{-6} J/cm^2 from the values of σ and $\sigma\sigma_e$. Cheng et al. also obtained $\sigma\sigma_e=5.9$–13.5×10^{-12} J^2/cm^4 by applying similar procedures [14]. In the previous paper, we obtained $\sigma_e=5.1\times 10^{-6}$ J/cm^2 of iPP from the slope of reliable Gibbs–Thomson plot [17]. Reliable σ can be obtained from the values of σ_e and $\sigma\sigma_e$ which will be obtained from the kinetic data of the present study.

The purpose of this paper is to clarify the M dependence of V of the α form crystals of iPP. The "power law" of M of V will be shown later in this paper. The universality of the "power law" suggests the topological nature of polymer crystallization. The side surface free energy σ of the α form crystals of iPP will also be determined from the kinetic data by using the reliable σ_e and T_m^0 obtained in the previous paper.

2. Experimental

Four iPP fractions with high tacticity were used in this study. Their characteristics are listed in Table 1. Number-averaged molecular weights (M_n) were 23×10^3, 64×10^3, 94×10^3

Table 1
Sample characteristics

Sample name	$M_n\times 10^{-3}$	$M_w\times 10^{-3}$	M_w/M_n	[mmmm] (%)	T_m^0 [a] (°C)
23K	23	51	2.2	99.6	183.7
64K	64	152	2.4	99.6	186.1
94K	94	230	2.4	99.6	186.4
263K	263	605	2.3	99.6	187.7

[a] Ref. [17].

and 263×10^3. They are named 23K, 64K, 94K and 263K, respectively. They were similar in molecular weight distribution ($M_w/M_n = 2.2–2.4$) and tacticity ([mmmm] = 99.6%), as shown in Table 1. The molecular weight and molecular weight distribution were measured by using gel permeation chromatography. The tacticity was estimated by means of ^{13}C nuclear magnetic resonance. Table 1 also shows the T_m^0 which was obtained by using Gibbs–Thomson plot in the previous paper [17].

Isothermal crystallization was carried out by using a hot stage, Mettler FP82, under nitrogen flow with 2 L/min. Crystallization behavior was observed by a polarizing optical microscope (OM), OLYMPUS BX-P, equipped with sensitive color plate. It was recorded on a videotape by using FLOVEL HC-3600 3CCD camera. Sample was put between slide glass and cover glass with a Cu spacer of 100 μm in thickness. Sample was melted at 220 °C for 5 min, and the isothermal crystallization was carried out at $T_c = 126–150$ °C. Observation of growing crystals was carried out in the middle depth of the melt to eliminate the influence of temperature gradient within the melt. Lateral size of crystal (a) was measured at the early stage of the formation of spherulite ($a < 30$ μm) and was defined as the length of the longest axis. V was defined as $V = (1/2)(da/dt)$, where t is the crystallization time.

3. Results

3.1. Morphology

Typical polarizing optical micrographs of crystals are shown in Fig. 1. For lower molecular weight fractions at high crystallization temperatures, a crystalline aggregate called, quadrite, was formed in the early stage of growth and grew into spherulite. The spherulites shown in Fig. 1 are the type II assigned by Norton and Keller [18] for the α form spherulites obtained at relatively high crystallization temperatures. The color pattern of retardation of the quadrite was the same as that of type II spherulite.

It is well known that iPP has a cross-hatched lamellar structure [19–21]. Olley and Bassett [20] observed the lamellar morphology of melt-crystallized quadrites by means of transmission electron microscopy. They showed that the origin of quadrites is the cross-hatched edge-on lamellae. The four corners of quadrite correspond to the growth fronts of the

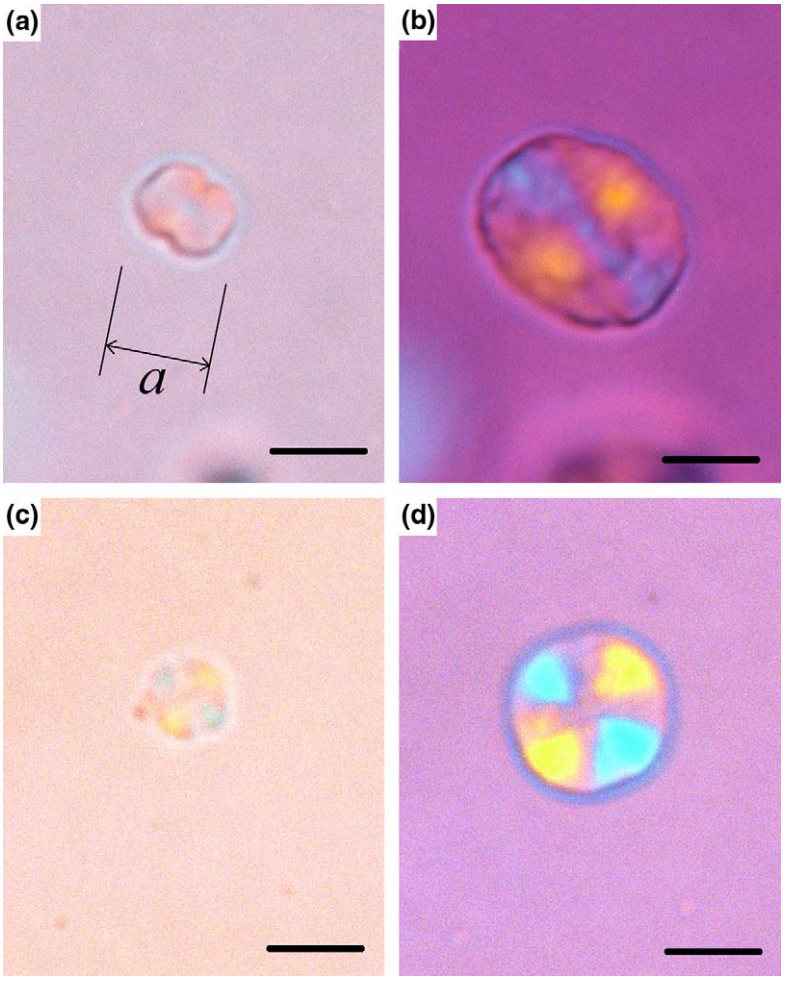

Fig. 1. Polarizing optical micrographs of crystals of 23K at 134 °C for (a) 84 and (b) 122 s and of 263K at 150 °C for (c) 43 and (d) 72 min. Scale bars represent 10 μm.

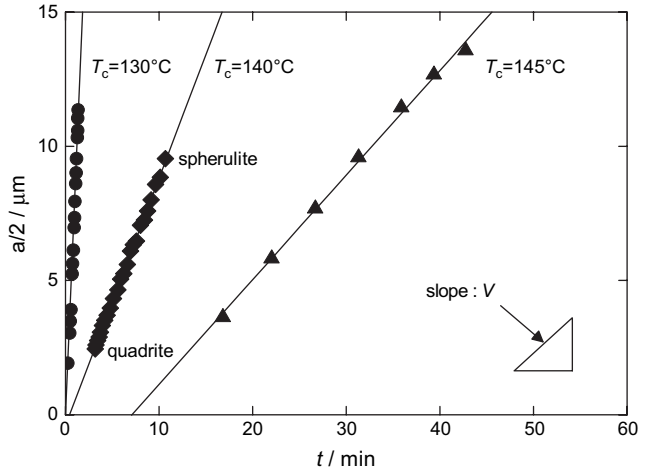

Fig. 2. Typical plots of $a/2$ against crystallization time, t, for different T_c of 23K fraction.

dominant lamellae of spherulite. Hence, the length along the longest axis of the quadrites defined as a in Fig. 1a corresponds to the diameter of the spherulites.

3.2. Steady lateral growth

Fig. 2 shows typical examples of the plots of $a/2$ against t for different T_c. The length, $a/2$, increased linearly with t, irrespective of M_n and T_c. The slope of the straight line of $a/2$ against t defines the rate of steady lateral growth, V. The morphological change from quadrite to spherulite did not affect the slope of the plot. It means that the growth mechanism, *i.e.*, the growth regime, of quadrite and spherulite must be the same.

3.3. TΔT dependence of V(M)

Fig. 3 shows the plots of Log(V) against T_c for different M_n. Based on Eqs. (1) and (5) with the empirical values of

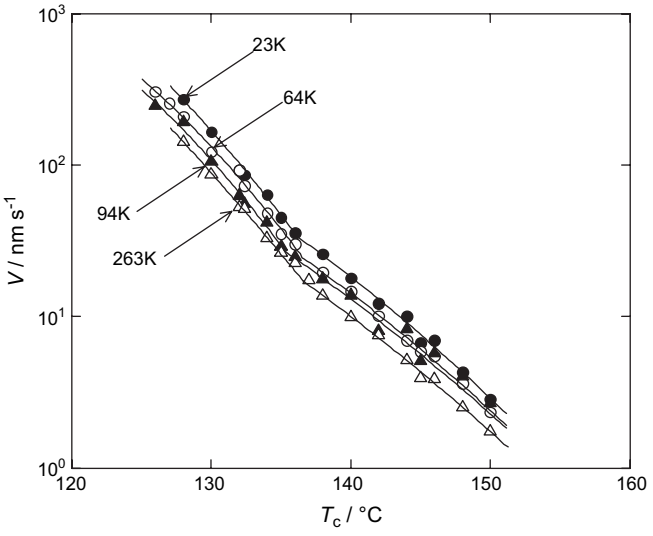

Fig. 3. Plots of V against crystallization temperature, T_c, for different M_n.

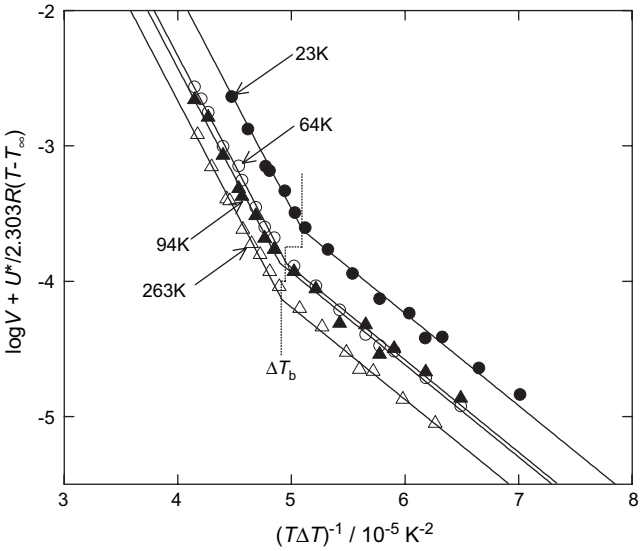

Fig. 4. Plots of $\mathrm{Log}(V) + U^*/2.303\mathrm{R}(T - T_\infty)$ against $(T\Delta T)^{-1}$.

$T_\infty = 231.2$K and $U^* = 1500$ cal/mol for iPP [13], $\mathrm{Log}(V) + U^*/2.303\mathrm{R}(T - T_\infty)$ are also plotted against $(T\Delta T)^{-1}$ in Fig. 4. Irrespective of M_n, the values decrease linearly with the increase in $(T\Delta T)^{-1}$, and the plots give almost parallel straight lines. Breakings of the lines are observed at about $\Delta T \cong 49$K ($= \Delta T_b$) for all samples. The breaking has been explained as the regime II–III transition by Clark and Hoffman [13]. Hence, we assume that the multi-nucleation regimes of II and III occur at $\Delta T < \Delta T_b$ and $\Delta T > \Delta T_b$, respectively. The slope of the lines in Fig. 4, B, is plotted against M_n in Fig. 5. It is indicated that B does not significantly depend on M_n in both regions below and above ΔT_b. The lines in Fig. 4 are drawn by using averaged B ($\overline{B}$),

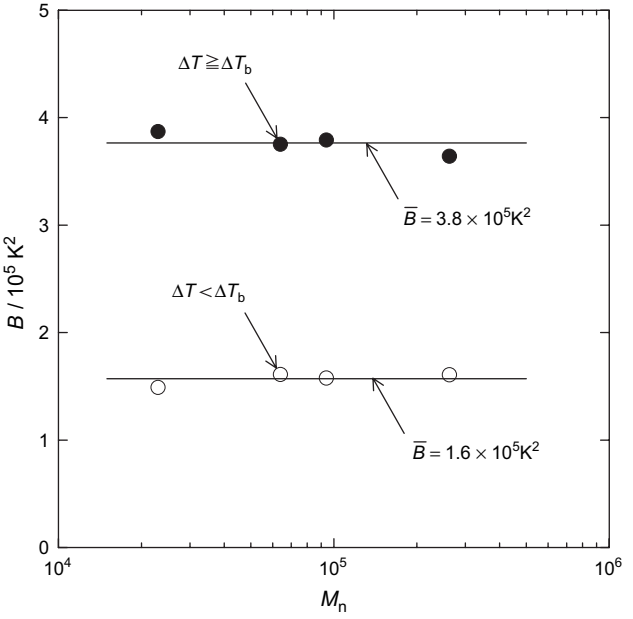

Fig. 5. The slope, B, of the plots in Fig. 4 plotted against M_n.

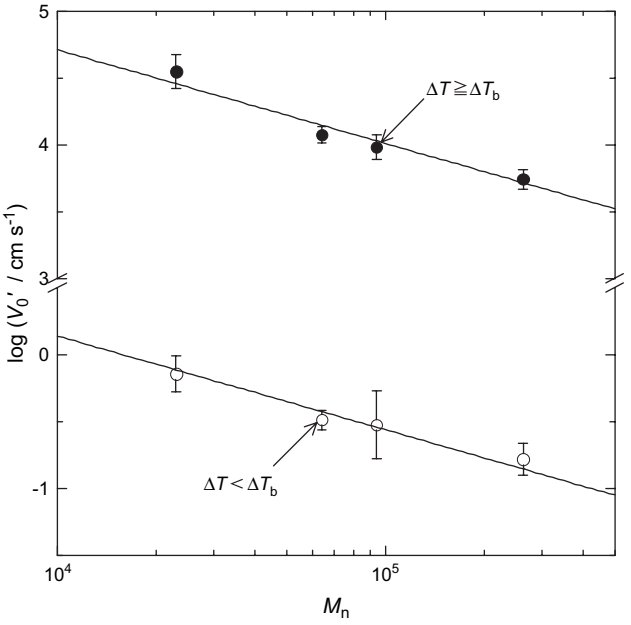

Fig. 6. The intercept, V_0', of the plots in Fig. 4 plotted against M_n.

$$\begin{aligned} \overline{B} &\cong 3.8\times 10^5 \quad \text{for } \Delta T > \Delta T_b = 49\text{K} \\ &\cong 1.6\times 10^5 \quad \text{for } \Delta T < \Delta T_b = 49\text{K} \end{aligned} \tag{9}$$

The ratio of B, 3.8/1.6 ≈ 2.4, is not far from the value of 2 expected for the regime II–III transition [13].

3.4. Power law of M dependence of V

The coefficient, V_0', of each M_n was obtained by the extrapolation of the plots in Fig. 4 to $(T\Delta T)^{-1} = 0$ by using the averaged slope of $\overline{B}$. Log(V_0') is plotted against Log Log(M_n) for below and above ΔT_b in Fig. 6. It is shown that Log(V_0') linearly decreases with the increase in Log(M_n). Thus, we have confirmed the power law of Eq. (7) with $H = 0.7$ for the helical polymer of iPP as the case of PE [3,4].

4. Discussion

4.1. Relation between H and chain sliding diffusion

It has been reported that the powers of PE are $H = 0.7$ and $H = 1.7$ for the hexagonal and orthorhombic phases of PE, respectively [3,4]. Therefore, the following relationship holds among the powers of H_{iPP}, H_{PE}(hexagonal), and H_{PE}(orthorhombic),

$$H_{iPP} \cong H_{PE}(\text{hexagonal}) < H_{PE}(\text{orthorhombic}) \tag{10}$$

Orthorhombic PE is regarded as a special polymer because of its ''planar-zigzag'' chain conformation. On the other hand, the chain conformation of hexagonal PE, which is regarded as a rod-like polymer due to chain rotation, is similar to that of helical polymers. Therefore, the present results confirm that the chain sliding becomes easier for helical polymers.

4.2. Lateral surface free energy

The Gibbs–Thomson equation is expressed as,

$$T_m(\ell) \cong T_m^0 - \frac{C}{\ell}, \tag{11}$$

$$C = \frac{2\sigma_e T_m^0}{\Delta h}. \tag{12}$$

where ℓ represents the crystal lamellar thickness. The following equations are obtained by the combination of Eqs. (4) and (12),

$$\sigma = \frac{mk}{2b_0}\frac{B}{C}. \tag{13}$$

Therefore, σ can be directly obtained by using Eq. (13) without Δh_f.

In the previous study, we obtained $C = 2.40\times 10^{-5}$ cm K [17]. As a result, σ was obtained as,

$$\sigma = 1.73\times 10^{-6}(\text{J/cm}^2) \quad \text{for } \Delta T > \Delta T_b = 49\text{K} \tag{14a}$$

$$= 1.44\times 10^{-6}(\text{J/cm}^2) \quad \text{for } \Delta T < \Delta T_b = 49\text{K}. \tag{14b}$$

and the averaged $\langle\sigma\rangle$ is

$$\langle\sigma\rangle = 1.59\times 10^{-6}(\text{J/cm}^2). \tag{15}$$

4.3. Effect of M_n dependence of melt viscosity

The mobility term of Eq. (5) depends on the glass transition temperature (T_g) through the empirical relationship between T_g and T_∞, $T_\infty = T_g - 30$K. The mobility and the glass transition temperature are determined by the free volume, which is dependent on molecular weight due to the effect of chain ends. The dependence is expressed as the Fox–Flory equation [22],

$$T_g = T_g^\infty - K/M_n, \tag{16}$$

where T_g^∞ is the T_g of infinite molecular weight and K is a positive constant. Therefore, we need to estimate the influence on the M_n dependence of V. The M_n dependence of T_g of polypropylene was studied by Cowie [23]. From the results, the following relationship between T_g and M_n of iPP was evaluated,

$$T_g = 267.9 - 32{,}398/M_n\ (\text{K}). \tag{17}$$

Accordingly, T_g of the present samples are estimated as follows; $T_g(M) = 266.5$, 267.4, 267.5 and 267.7 °C for 23K, 64K, 94K and 263K, respectively.

From the dependence, the following approximate expansion is obtained,

$$\frac{1}{T - T_\infty} \cong \frac{1}{T - T_\infty^\infty}\left(1 - \frac{K}{T - T_\infty^\infty}M_n^{-1}\right), \tag{18}$$

where T_∞^∞ is the T_∞ of infinite molecular weight. On the other hand, in terms of the M_n dependence of the effective activation

energy, U^*, it is believed that the fragility parameter, *i.e.*, the apparent activation energy of the conformational relaxation time, τ, *i.e.*, $-\mathrm{d}\log\tau/\mathrm{d}(T_g/T)\approx U^*/\mathrm{R}T_g$, is determined only by the molecular species and not influenced by the chain length [24]. Therefore, the M_n dependence of U^* is expected to be similar to that of T_g. Due to the M_n dependences of T_g and U^*, the exponential term in Eq. (5) is modified as,

$$\exp\left[-\frac{U^*}{\mathrm{R}(T-T_\infty)}\right] \cong \exp\left[-\frac{U^*}{\mathrm{R}\left(T-T_\infty^\infty\right)}\right] \times \exp\left[\frac{U^*K}{\mathrm{R}\left(T-T_\infty^\infty\right)}\left(\frac{1}{T-T_\infty^\infty}+\frac{1}{T_g^\infty}\right)M_n^{-1}\right] \quad (19)$$

the second term in the right hand side of Eq. (19) represents the M_n dependence. The change in this term for the molecular weight range of the present samples is at most 5%, which will be negligible in comparison with the change of 450% expected from the power law dependence of V_0' on M_n.

5. Conclusion

(1) We have examined the molecular weight dependence of the linear growth rate of isotactic polypropylene, based on the relationship expressed as $V = V_0' \exp[-U^*/\mathrm{R}(T_c - T_\infty)]\exp[-B/T\Delta T]$. We have confirmed that V_0' decreases with the increase in M_n, while the first exponential term and B does not significantly depend on M_n.

(2) The M_n dependence of V_0' was expressed as, $V_0' \propto M_n^{-H}$, where $H = 0.7$. Thus, the power law for stereoregular polymer was confirmed. The power H of iPP (0.7) was close to the value (0.7) of the hexagonal phase of PE and smaller than that (1.7) of the orthorhombic phase of PE. The small H of iPP and of the hexagonal phase of PE must be caused by the loose packing of chains within the interface between the crystalline phase and the melt due to easier chain sliding.

(3) Lateral surface free energy $\sigma = 1.59 \times 10^{-6}$ J/cm^2 of the α form of iPP was obtained from the present kinetic data by using T_m^0 and σ_e determined from reliable Gibbs–Thomson plot.

Acknowledgements

The authors are very grateful to Dr. Jun-ichiro Washiyama of SunAllomer Ltd. for his encouraging supports. The authors also thank Dr. Shinichi Yamazaki of Okayama University for his helpful advices.

References

[1] Hikosaka M. Polymer 1987;28:1257.
[2] Hikosaka M. Polymer 1990;31:458.
[3] Nishi M, Hikosaka M, Toda A, Takahashi M. Polymer 1998;39:1591.
[4] Okada M, Nishi M, Takahashi M, Matsuda H, Toda A, Hikosaka M. Polymer 1998;39:4535.
[5] Ghosh SK, Hikosaka M, Toda A, Yamazaki S, Yamada K. Macromolecules 2002;35:6985.
[6] Nishi M, Hikosaka M, Ghosh SK, Toda A, Yamada K. Polym J 1999; 31:749.
[7] Vogel H. Phys Z 1921;22:645.
[8] Fulcher GS. J Am Ceram Soc 1925;8:339.
[9] Williams ML, Landel RF, Ferry JD. J Am Ceram Soc 1955;77:3701.
[10] Hoffman JD, Frolen LJ, Ross GS, Lauritzen Jr JI. J Res Natl Bur Stand 1975;79A:671.
[11] Flory P, Vrij A. J Am Chem Soc 1963;85:3548.
[12] Wunderlich B. Macromolecular physics. Academic Press; 1980.
[13] Clark EJ, Hoffman JD. Macromolecules 1984;17:878.
[14] Cheng SZD, Janimak JJ, Zhang A. Macromolecules 1990;23:298.
[15] Yamada K, Hikosaka M, Toda A, Yamazaki S, Tagashira K. Macromolecules 2003;36:4790.
[16] Yamada K, Hikosaka M, Toda A, Yamazaki S, Tagashira K. Macromolecules 2003;36:4802.
[17] Yamada K, Hikosaka M, Toda A, Yamazaki S, Tagashira K. J Macromol Sci B Phys 2003;B42:733.
[18] Norton DR, Keller A. Polymer 1985;26:704.
[19] Binsbergen FL, De Lange BGM. Polymer 1968;9:23.
[20] Olley RH, Bassett DC. Polymer 1989;30:399.
[21] Yamada K, Matsumoto S, Tagashira K, Hikosaka M. Polymer 1998;39: 5327.
[22] Fox TG, Flory PJ. J Appl Phys 1950;21:581.
[23] Cowie JMG. Eur Polym J 1973;9:1041.
[24] Roland CM, Ngai KL. Macromolecules 1992;25:5765.